# Sometimes It Takes Two to Tango: Contributions of Dimerization to Functions of Human α-Defensin HNP1

**Marzena Pazgier[†¶1], Gang Wei[†§1], Bryan Ericksen[†1], Grace Jung[¥], Zhibin Wu[†], Erik de Leeuw[†], Weirong Yuan[†], Henryk Szmacinski[‡], Wei-Yue Lu[§], Jacek Lubkowski[¶], Robert I. Lehrer[¥], and Wuyuan Lu[†‡*]**

[†]Institute of Human Virology and [‡]Department of Biochemistry and Molecular Biology, University of Maryland School of Medicine, 725 West Lombard Street, Baltimore, MD 21201; [¶]Macromolecular Assembly Structure and Cell Signaling Section, NCI, National Institutes of Health, Frederick, Maryland 21702; [§]School of Pharmacy, Fudan University, Shanghai 201203, China; [¥]Department of Medicine, David Geffen School of Medicine, UCLA, 10833 LeConte Ave., Los Angeles, CA 90095. [1]Equally contributing authors. [*]Author to whom correspondence should be addressed: wlu@ihv.umaryland.edu, Tel (410)706-4980; Fax (410)706-7583.

**Structural studies of HNP1 mutants.** Crystals of MeIle20-HNP1 and $(CGG\text{-}HNP1)_2$ were grown at room temperature using the hanging-drop, vapor diffusion method. Initial screenings were either done manually or robotically with the commercially available crystallization Sparse Matrix Screens from Hampton Research. For each of three proteins, equal volumes (0.5 μl) of defensin solution (20 mg/ml in water) and mother liquor solution were mixed and placed over 0.8 mL of reservoir solution. Crystals of MeIle20-HNP1 and $(CGG\text{-}HNP1)_2$ could be frozen for X-ray experiments directly from the droplets.

| HNP1 derivative | **Reservoir solution** |
|---|---|
| MeIle20-HNP1 | 0.1 M Na Hepes, pH 7.5; 0.2 M Na citrate, 30% MPD |
| $(CGG\text{-}HNP1)_2$ | 0.1 M Na citrate pH 5.6, 0.2 M NH4 acetate, 30% MPD |

X-ray diffraction data for MeIle20-HNP1 and $(CGG\text{-}HNP1)_2$ were collected using synchrotron radiation at the SER-CAT sector 22 beamlines of the Advanced Photon Source (Argonne, IL, USA) equipped with MAR225 or MAR300 CCD detectors. Data were integrated and scaled with HKL2000 (1). The statistics appear in **Table S1**. All structures were solved using the molecular replacement method as implemented in the program Phaser from the CCP4 suite (2). The monomer of HNP1 (PDB code 3GNY) or HNP3 (PDB code 1DFN) was used as a search model. Structural refinements were performed using the Refmac program (3) coupled with a manual refitting and rebuilding with the COOT program (4). The refinement statistics are summarized in **Table S1**. Due to the high similarity between tertiary structures of every mutant and HNP1, it is not surprising that very clear solutions were determined easily. In all cases, the log-likelihood (LLG) and the Z-score values for the complete solutions (i.e. containing two molecules present in the asymmetric units) were above 2,000 and 20, respectively. The structural features, specific to each model (i.e. N-MeIle20 or $(CGG)_2$-linker) could be clearly and unambiguously identified in the electron density difference maps, calculated from the initial phases. Coordinates and structure factors have been deposited in the PDB with accession codes 3HJD and 3HJ2 for MeIle20-HNP1 and $(CGG\text{-}HNP1)_2$, respectively. Molecular graphics were generated using Pymol (http://pymol.org) and Ribbons (5).

Crystals of $(CGG\text{-}HNP1)_2$ analog diffracted to a very-high resolution of 1.1 Å when exposed to the synchrotron radiation, and a complete dataset was collected. Despite an unambiguous solution of the structure of this mutant, however, the structure refinement statistics were rather unsatisfactory. When refinement was extended to the highest resolution range values of R-factor and free-R were about 0.20 and 0.23, respectively. Significantly, the electron density maps were amazingly clear, i.e. the positive and negative $F_o–F_c$ peaks clearly indicated inaccurately modeled fragments of the molecule and sites of the solvent, respectively, during the model improvement stage. At the end of refinement, the electron density $2F_o–F_c$ map correlated well with all atoms included in the model and no $F_o–F_c$ peaks were present for contouring below the -3σ level or above the 3σ level. Here, we are presenting the model of (CGG-

$HNP1)_2$, refined against the data limited to the resolution range of 1.4 Å and the data collection statistics describing such a limited data subset. Reducing the X-ray data to the range narrower than nominally achievable explains somewhat unusual values for such data collection statistics as $I/\sigma(I) = 17.7$ and $R_{merge} = 0.108$ for the highest reported resolution shell.

**Table S1**. X-ray data collection and refinement statistics for HNP1 mutants

| | **MeIle20-HNP1** | **$(CGG\text{-}HNP1)_2$** |
|---|---|---|
| Space group | P622 | $P2_12_12$ |
| Cell parameters, Å | a=b=69.85, c=46.33 | a=47.07, b=49.37, c=24.99 |
| Molecules/a.u. | 2 | 2 |
| Resolution, Å | 30-1.65 (1.71-1.65) | 40-1.40 (1.45-1.40) |
| No. unique reflections | 8,402 | 11,611 |
| $R_{merge}$[b], % | | |
| Completeness, % | 10.8 (55.7) | 5.3 (10.8) |
| Redundancy | 99.4 (99.5) | 96.3 (100.0) |
| I/σ(I) | 13.0 (11.0) | 6.2 (6.4) |
| | 16.4 (4.2) | 22.5 (17.7) |
| | **MeIle20-HNP1** | **$(CGG\text{-}HNP1)_2$** |
| Resolution, Å | 20-1.65 | 15-1.40 |
| R[c], % | 17.5 | 19.9 |
| $R_{free}$[d], % | 203 | 23.6 |
| No. protein atoms | 482 | 487 |
| No. non-protein atoms | | |
| Water | 73 | 51 |
| Ligands | 0 | 0 |
| **RMS deviations** | | |
| Bond lengths, Å | 0.019 | 0.020 |
| Bond angles, ° | 2.01 | 1.86 |
| **Ramachandran plot** | | |
| Most favored region, % | 95.8 | 96 |
| Additional allowed | 4.2 | 4 |
| Generously allowed | 0 | 0 |
| Disallowed | 0 | 0 |

[a]All data (outer shell).
[b]$R_{merge} = \sum|I - \langle I\rangle|/\sum I$, where $I$ is the observed intensity and $\langle I\rangle$ is the average intensity obtained from multiple observations of symmetry-related reflections after rejections
[c]$R = \sum||F_o| - |F_c||/\sum|F_o|$, where $F_o$ and $F_c$ are the observed and calculated structure factors, respectively
[d]$R_{free}$ = defined by (6)

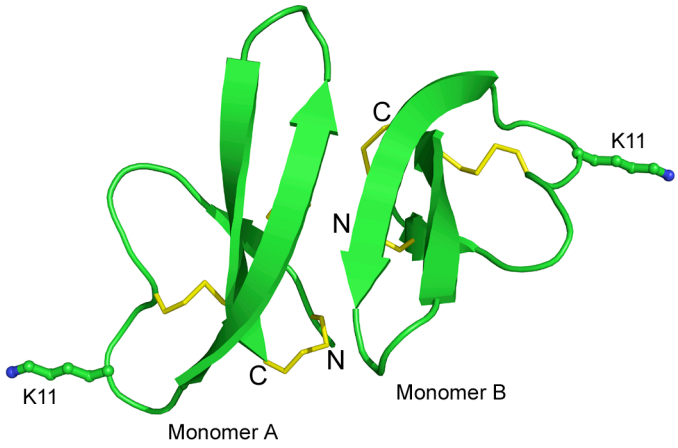


**Figure S1**. A hypothetical model of A11K-HNP1 based on the crystal structure of wild type HNP1. The two Lys-11 side chains in the dimer structure are shown in sticks, and the distance between the two Cα atoms of residue 11 is 33.5 Å.

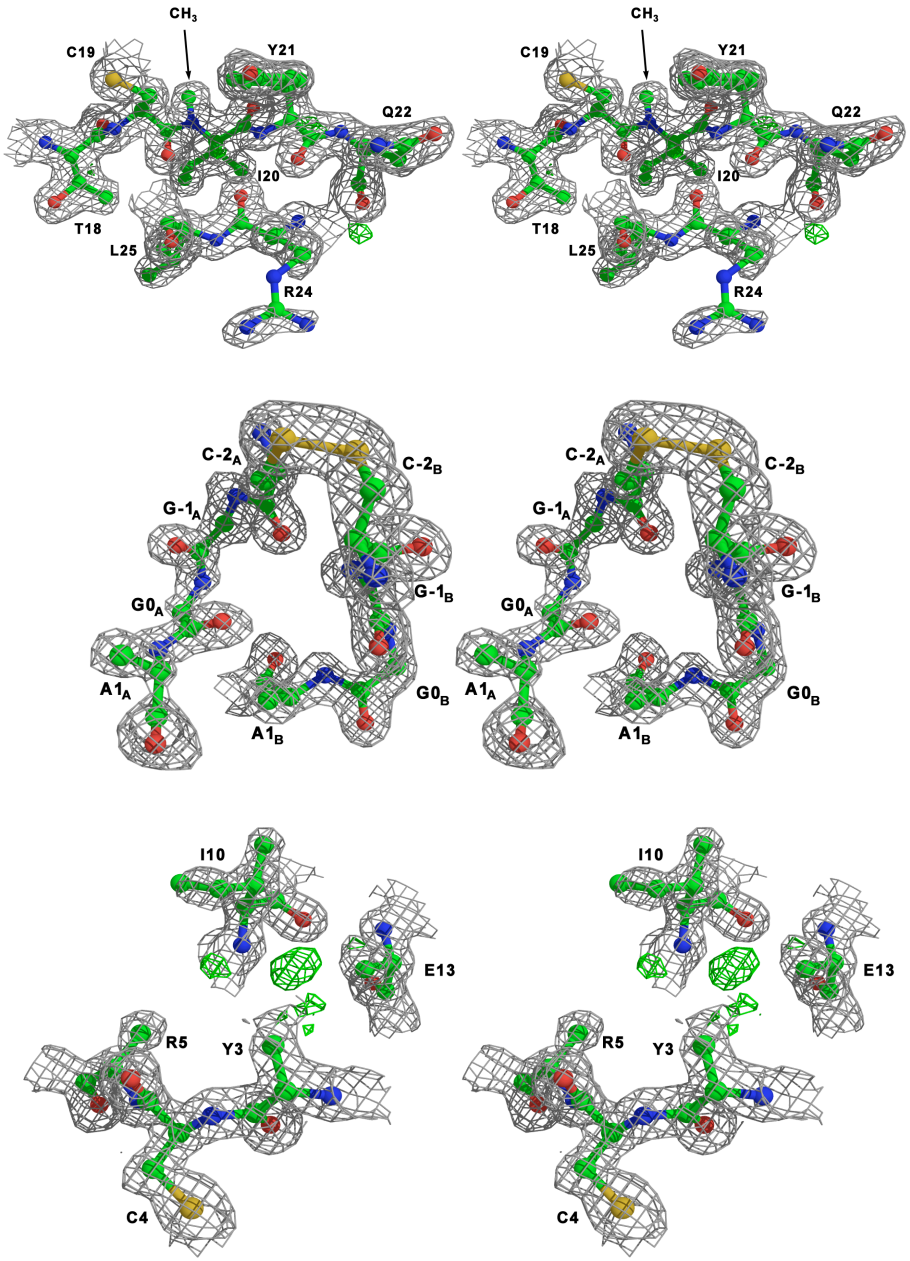


**Figure S2.** (**A**) Stereo representation of the electron density around the N-methylated Ile20 in the structure of MeIle20-HNP1. The $2F_o–F_c$ electron density map (shown in gray) was contoured at 1σ level and the $F_o–F_c$ peaks contoured at +3σ are colored in green (the $F_o–F_c$ peaks contoured at -3σ are absent in this area of the model). The methyl group attached to the peptide nitrogen atom of Ile20 is well defined in the electron density. (**B**) Stereo representation of the electron density for the $(CGG)_2$-linker in the structure of the $(CGG\text{-}HNP1)_2$ analog. The $2F_o–F_c$ electron density map shown in gray was contoured at 1σ level. For this fragment of the model, no $F_o–F_c$ peaks are present at either -3σ or +3σ contouring levels. (**C**) Stereo representation of the electron density for the region of three disordered residues in the monomer A of the $(CGG\text{-}HNP1)_2$ analog. The $2F_o–F_c$ electron density map shown in gray was contoured at 1σ level. Three disordered residues: Tyr3, Arg5, and Glu13 were represented by alanine residues since the $F_o–F_c$ electron density map (shown here in green and contoured at 3σ level) did not allow for an unambiguous modeling of the side chain for these residues.

**References:**


1. Otwinowski Z & Minor W (1997) *Methods Enzymol*. 276:307-326.
2. Storoni LC, McCoy AJ, & Read RJ (2004) Likelihood-enhanced fast rotation functions. *Acta Crystallogr D Biol Crystallogr* 60(Pt 3):432-438.
3. Murshudov GN, Vagin AA, & Dodson EJ (1997) Refinement of macromolecular structures by the maximum-likelihood method. *Acta Crystallogr D Biol Crystallogr* 53(Pt 3):240-255.
4. Emsley P & Cowtan K (2004) Coot: model-building tools for molecular graphics. *Acta Crystallogr D Biol Crystallogr* 60(Pt 12 Pt 1):2126-2132.
5. Carson M (1991) Ribbons 2.0. *J Appl Cryst* 24:958-961.
6. Brunger AT (1992) Free R value: a novel statistical quantity for assessing the accuracy of crystal structures. *Nature* 355(6359):472-475.